

Simulation of Fracture Healing Using Cellular Automata*

(Influence of Operation Conditions on Healing Result in External Fixation)

Shozo KAWAMURA**, Kazunori KAMITANI**, Takuzo IWATSUBO**,
Mitsumasa MATUDA**, Masahiro KUROSAKA**, Shinichi YOSHIYA**,
Hirotsugu MURATSU** and Eberhard P. HOFER**

In this study, fracture healing was simulated by the CA method, which is one of the discrete computation methods. First, the state of a cell was defined as “bone”, “cartilage” or “fibrous connective tissue” and a set of local rules was constructed referring to the fuzzy logic model for sheep metatarsal. The simulation results obtained by the CA method agreed well with the ones in the previous research and the experimental data. As a result, it was concluded that the CA simulation model proposed in this study is a suitable model for describing fracture healing. Next, modifying the parameters of local rules, fracture healing of human bone was simulated. On the basis of the simulation results obtained under various conditions of external fixation, it was concluded that an optimal set of stopper gap and initial gap conditions may exist because they have a close relationship to each other.

Key Words: Biomechanics, Computational Mechanics, Finite Element Method, Fracture Healing, Cellular Automata, External Fixation

1. Introduction

Bone is assumed to be an adaptive material that is capable of changing its structure under external loads in order to establish physiological loading conditions inside the tissue. In the case of fracture treatment by external fixation, appropriate loading will facilitate the healing result. There have been some computer simulations on fracture healing. Carter et al.^{(1),(2)} and Blenman et al.⁽³⁾ considered finite element analysis of a fracture callus at different stages of ossification. Their results suggest that the stresses in tissue influence the revascularization and tissue differentiation. Prendergast et al.⁽⁴⁾ inferred that the fluid velocity in tissues regulated tissue differentiation. Claes et al.^{(5),(6)} investigated the effects of local mechanical stimuli, i.e., local stress and strain, on tissue differentiation using the finite element model. Alicia et al.⁽⁷⁾ investigated the effects of mechanical stimulation on cell differentiation and ossification. Lacroix and Prendergast⁽⁸⁾ simulated the tissue differentiation during fracture healing using the finite element model and investigated the effects of gap size and loading magnitude on a interfragmentary move-

ment. Gardner et al.⁽⁹⁾ investigated the influences of a mechanical stimulus on the pattern of tissue differentiation and the maturation of the callus using the finite element method, and they calculated the stress concentration and mechanical failure of human tibia using the finite element model⁽¹⁰⁾. Duda et al.^{(11),(12)} investigated the effects of interfragmentary movement on fracture healing by computer simulation. One of the present authors proposed a fuzzy logic model of fracture healing⁽¹³⁾ in which three types of tissue, bone, cartilage and fibrous connective tissue, were used and a set of fuzzy rules derived from medical knowledge was implemented to describe time transformation. The results showed good agreement with the actual measured data.

On the other hand, some of the present authors proposed a cellular automata (CA) model of bone remodeling under external loads⁽¹⁴⁾. The CA method is one of the discrete computation methods. The analytical domain is divided into finite state variables called ‘cells’. The state of each cell is updated according to local rules at every discrete time step. That is, the state of a cell at a given time step depends only on its previous state and that of neighbor cells. States of all cells are updated synchronously. Because of such computational characteristics, analysis can be performed for only a desired portion of total space. A local rule is designed in such a way that the results will sat-

* Received 23rd February, 2004 (No. 04-4062)

** Department of Mechanical Engineering, Toyohashi University of Technology, 1-1 Tempaku, Toyohashi 441-8580, Japan. E-mail: kawamura@mech.tut.ac.jp

isfy the requirements. In our study, five types of state, i.e., bone marrow, osteoclast, osteoblast, bone cell and osteoprogenitor cell, are adopted and the metabolism rule and bone formation rule are used to update the states of cells. The results showed good agreement with the actual bone density distribution.

In this study, the CA method for simulating the fracture healing during external fixation is proposed and the optimal condition for external fixation is obtained. Because the mechanism of fracture healing is not yet completely elucidated, we will refer to the basic idea of tissue transformation presented in the previous paper⁽¹³⁾, which yields adequate results. Each cell is in one of the bone, cartilage or fibrous connective tissue states, and a set of local rules is constructed referring to fuzzy logic. In the first step of this study, fracture healing during external fixation of sheep metatarsal is simulated and the validity of the method proposed in this paper will be checked in comparison with the actual measured data. Next, fracture healing of human bone is simulated and the influences of the operating conditions on the healing result will be evaluated.

2. Outline of Fuzzy Logic Model

In this section, the outline of the previous study⁽¹³⁾ is described. Fracture healing during external fixation of sheep metatarsal is treated. In the study, the finite element method is used so that the analytical domain is divided into some finite elements. Three types of tissue, i.e., bone, cartilage and fibrous connective tissue are considered and the proportion of each tissue in one finite element, i.e., μ_{Bone} , $\mu_{\text{Cartilage}}$ and $\mu_{\text{ConnTissue}}$, is updated on the basis of the fuzzy logic. Fibrous connective tissue includes all other tissues except bone and cartilage. The update process is described below. For one finite element, strain energy density u and osteogenic factor c , which indicates the ease of transformation to bone, are defined. The values u and c under external load are calculated by the finite element method and they are evaluated using the membership function. That is, the strain energy density is classified into four fuzzy sets {low, physiologic, increased, pathologic} and the degree of each set is represented by $\mu_{u(\text{low})}$, $\mu_{u(\text{physiologic})}$, $\mu_{u(\text{increased})}$ and $\mu_{u(\text{pathologic})}$. The osteogenic factor is also classified into two fuzzy sets {poor, high} and the degree of each set is represented by $\mu_{c(\text{poor})}$ and $\mu_{c(\text{high})}$. An example of a fuzzy rule is as follows.

IF $\mu_{\text{ConnTissue}}$ AND $\mu_{c(\text{high})}$ AND $\mu_{u(\text{physiologic})}$ THEN intramembraneous ossification.

Seven fuzzy rules, like that above are defined, according to which the proportions of the three types of tissue in one finite element change. The details of the simulation can be found in the previous paper⁽¹³⁾.

3. Fracture Healing Simulation of Sheep Metatarsal by CA Method

In this section, fracture healing during external fixation of sheep metatarsal is simulated and the validity of the method proposed in this paper will be checked by comparison with the actual measured data.

3.1 Methods

The state of a cell is defined as “bone”, “cartilage” or “fibrous connective tissue”.

When one cell is the same size as the actual tissue and it is one element in the finite element analysis, a huge number of cells is needed to model the fracture so the finite element analysis cannot be performed. In this study, one element for finite element analysis is divided into small cells in order to apply the CA method. As shown later, one element is divided into 400 cells in this study.

The local rules used to update the state in this study are explained. The strain energy density u is defined as

$$u = (1/2)\{\varepsilon\}^T \cdot \{\sigma\}, \quad (1)$$

where

$$\begin{aligned} \{\varepsilon\} &= \{\varepsilon_x \ \varepsilon_y \ \varepsilon_z \ \varepsilon_{xy} \ \varepsilon_{yz} \ \varepsilon_{xz}\}^T, \\ \{\sigma\} &= \{\sigma_x \ \sigma_y \ \sigma_z \ \tau_{xy} \ \tau_{yz} \ \tau_{xz}\}^T. \end{aligned} \quad (2)$$

In the previous paper, u was classified into four fuzzy sets and the membership functions for the sets crossed at $u = 0.5, 2.0$ and 35.5 [$\mu\text{J}/\text{mm}^3$]. Referring the membership functions, μ_u is set as follows.

$$\begin{aligned} \text{If } u < 0.5 & \quad \text{then } \mu_u: \text{low} \\ \text{If } 0.5 \leq u < 35.5 & \quad \text{then } \mu_u: \text{physiologic} \\ \text{If } 35.5 \leq u & \quad \text{then } \mu_u: \text{pathologic} \end{aligned} \quad (3)$$

The osteogenic factor c is evaluated by checking for the presence of bone cells in the surroundings.

Table 1 shows a set of local rules. “Conn.Tissue” refers to the fibrous connective tissue. The variable “Rate” means that that number of cells of the rate is selected randomly from the candidate cells to change and these cells are changed at the time step. The values of “Rate” are set referring to the previous paper⁽¹³⁾.

Here, the analytical model is explained. Fracture healing of sheep metatarsal is simulated. A longitudinal section of the fracture part is shown in Fig. 1 (a). In the fracture part, there is a gap of L because of the presence of intercalary tissue. The external fixator is attached to hold the fracture part and compressive load is applied by springs. In the early stage of healing, the gap is limited to D_{max} by a stopper to protect the new tissue in the growth process. In this section, the initial gap L is 3.0 mm and stopper gap D_{max} is 1.3 mm.

The analytical domain is shown in Fig. 1 (b). On the left-hand side of the domain, the horizontal displacement is constrained, while on the bottom side, the perpendicular

Table 1 Local rules for bone healing

Phenomenon	Local rule	Rate (%/days)
Intramembraneous Ossification	“Conn.Tissue” changes to “Bone” when the stimulus belongs to “high” and there are some “Bone” cells in the surroundings.	1
Chondrogenesis	“Conn.Tissue” changes to “Cartilage” when the stimulus belongs to “high” and there are no “Bone” cells in the surroundings.	5
Chondral ossification	“Cartilage” changes to “Bone” when the stimulus belongs to “high” and there are some “Bone” cells in the surroundings.	2
Atrophy of cartilage	“Cartilage” changes to “Conn.Tissue” when the stimulus belongs to “low”.	8
Destruction of Cartilage	“Cartilage” changes to “Conn.Tissue” when the stimulus belongs to “pathlogic”.	4
Atrophy of bone	“Bone” changes to “Conn.Tissue” when the stimulus belongs to “low”.	20
Destruction of bone	“Bone” changes to “Conn.Tissue” when the stimulus belongs to “pathlogic”.	10

displacement is constrained. In this domain there are 8 099 nodes and 15 840 triangular elements. Finite element analysis is performed as a two-dimensional plane strain problem.

The material properties of tissues⁽¹³⁾ are shown in Table 2. One rectangular element, which consists of two triangular elements, is divided into 400 cells. The strain energy density is the average of the values for the two triangular elements.

Young’s modulus E and Poisson’s ratio ν are determined according to the rates of the three types of state as follows:

$$\begin{aligned}
 E &= (E_{\text{Bone}} \times a_{\text{Bone}} + E_{\text{Cartilage}} \times a_{\text{Cartilage}} \\
 &\quad + E_{\text{ConnTissue}} \times a_{\text{ConnTissue}}) / 400 \\
 \nu &= (\nu_{\text{Bone}} \times a_{\text{Bone}} + \nu_{\text{Cartilage}} \times a_{\text{Cartilage}} \\
 &\quad + \nu_{\text{ConnTissue}} \times a_{\text{ConnTissue}}) / 400,
 \end{aligned}
 \tag{4}$$

where $a_{(\cdot)}$ indicates the number of (\cdot) in one rectangular element.

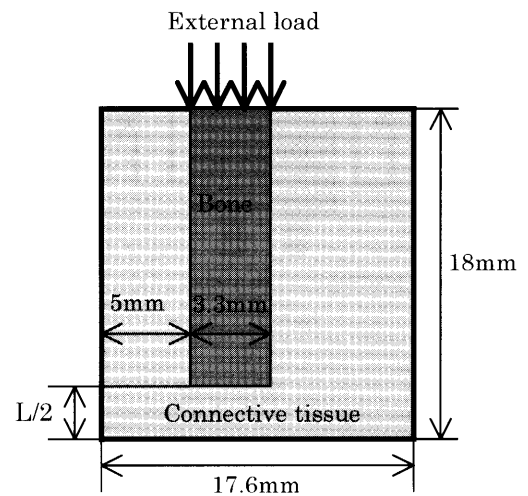
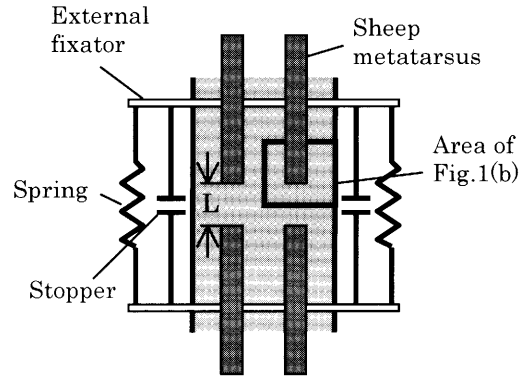


Fig. 1 Sheep metatarsal with external fixation

Table 2 Properties of tissues for sheep

Tissue	Modulus of elasticity E [MPa]	Poisson’s ratio ν
Bone	4000	0.3
Cartilage	40	0.35
Connective tissue	0.5	0.45

The process of the analysis is as follows. The compressive load applied by the springs, as shown in Fig. 1 (b), is set at 500 N ($= F_{\text{max}}$) which is the effective load to one leg of the sheep⁽¹³⁾. In the healing process, the reaction force caused by the growth of new tissues increases so that the deformation does not exceed the stopper gap.

The analytical process before deformation exceeds the stopper gap is as follows. When the load F_{max} acts on the upper surface, the deformation of the upper surface is calculated by the finite element method. If the growth of new tissue is not sufficient, the deformation exceeds D_{max} so that the external load is adjusted such that the deformation is equal to D_{max} . The finite element analysis is then performed under the adjusted load, and the strain energy density of every element is calculated. After that, the strain energy density and the presence of bone in the sur-

roundings of each cell are checked and the state of the cell is changed according to the local rule in Table 1. Young's modulus and Poisson's ratio of each cell after the change of state are calculated by Eq. (3), then finite element analysis is repeated.

After the deformation no longer exceeds the stopper gap, the finite element analysis is performed and the strain energy is calculated. The state of each cell is then changed according to the local rule in Table 1.

3.2 Simulation results and discussion

The simulation results for the modulus of elasticity are shown in Fig. 2. In the early stage of healing, we can observe a higher modulus of elasticity than that of the connective tissue over a wide area. This means that the external load is supported by a wide area. New bone is then generated in the gap, and after about 60 days after operation, the gap is filled by bone. After that, the tissue around the bone gradually changes to connective tissue. These results agree well with the ones in the previous paper⁽¹³⁾.

The deformation of the osteotomy gap is shown in Fig. 3. In the first stage of healing, the displacement is constrained by stoppers to the value of 1.3 mm. After about 70 days, the deformation is almost constant so that the bone fracture is considered to have almost healed in the

clinical sense. The deformation indicates the static deformation of normal bone under external load and the value is 9.85×10^{-3} mm.

The validity of the simulation is checked. The displacements of the osteotomy gap in this study, the previous study⁽¹³⁾ and the actual measured data⁽¹³⁾ are compared. The results are shown in Fig. 4, the result of this simulation agrees well with the actual measured data.

On the basis of the above results, it is concluded that the CA simulation model proposed in this study is a suit-

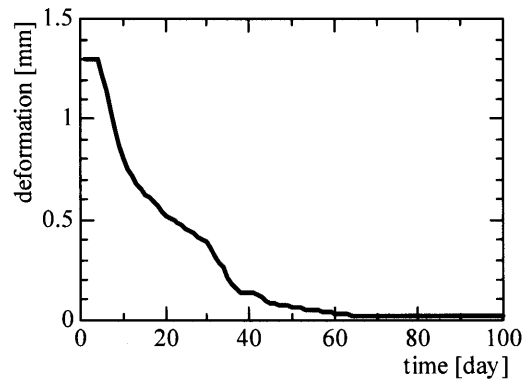


Fig. 3 Static deformation of the osteotomy gap

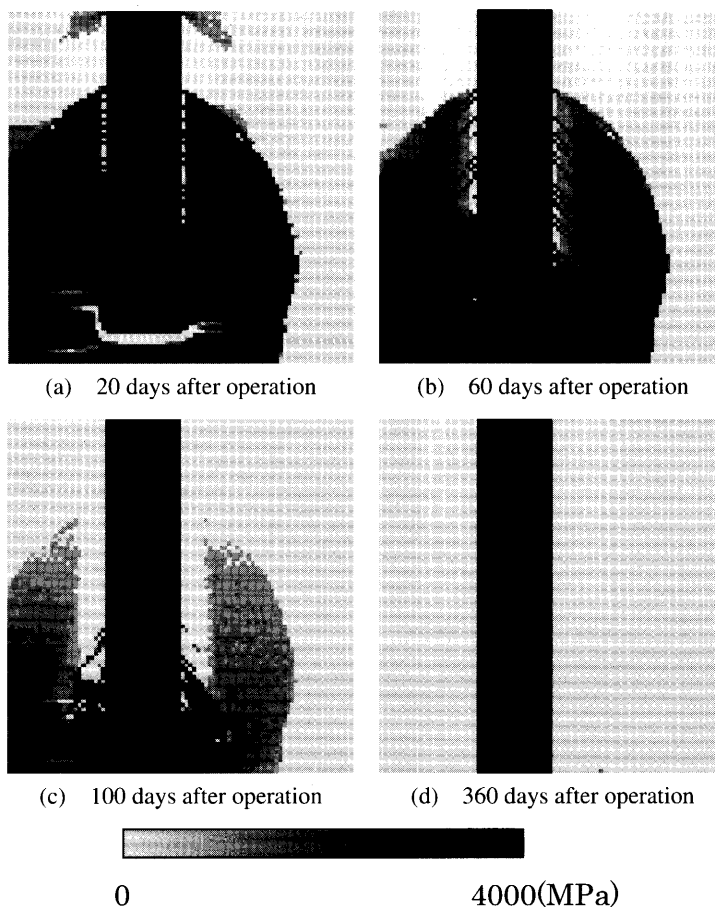


Fig. 2 Modulus of elasticity at sequential stages of fracture healing

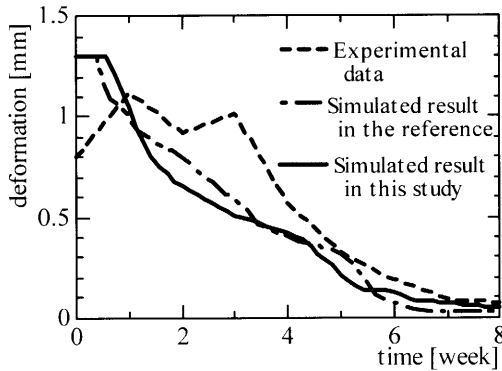


Fig. 4 Comparison of the deformation of the osteotomy gap among animal experiment, simulation in the Ref. (13) and the one in this paper

able model for describing fracture healing.

4. Fracture Healing Simulation of Human Bone by CA Method

4.1 Methods

In this section, the simulation method described in the previous section will be applied for the healing of human bone. The influences of the operating conditions on the healing results are investigated. The external fixation shown in Fig. 1 (a) is considered, and the size of the simulation domain is shown in Fig. 5. This domain is divided into 33 800 triangular elements with 17 161 nodes. The material properties of human tissue⁽¹⁵⁾ are shown in Table 3. Young's modulus and Poisson's ratio are determined using Eq. (4). The initial gap L and the stopper gap D_{\max} are set to be $L = 3.0$ mm and $D_{\max} = 0.2$ mm, respectively, in the reference case. F_{\max} is set to be 600 N, which is the effective load for humans.

The strain energy density factor μ_u is modified for the human case as follows.

$$\begin{aligned} \text{If } u < 0.04 & \quad \text{then } \mu_u: \text{ low} \\ \text{If } 0.04 \leq u < 20.0 & \quad \text{then } \mu_u: \text{ physiologic} \\ \text{If } 20.0 < u & \quad \text{then } \mu_u: \text{ pathologic} \end{aligned} \quad (5)$$

These factors are determined by trial and error so as to obtain valid results that agree with those for actual cases under reference conditions. The simulation procedure is the same as that in section 3.1.

4.2 Simulation results for reference model

The results are shown in Figs. 6 and 7. Figure 6 shows the distribution of Young's modulus during the healing process, and it shows that the gap is replaced by bone in proportion to time. Figure 7 shows that the static deformation of the upper surface with external load F_{\max} decreases as bone growth progresses.

The simulations for various cases of initial gap L and stopper gap D_{\max} are performed and the results are compared. First, complete healing is defined. Complete healing in this study does not mean perfect healing, i.e., the

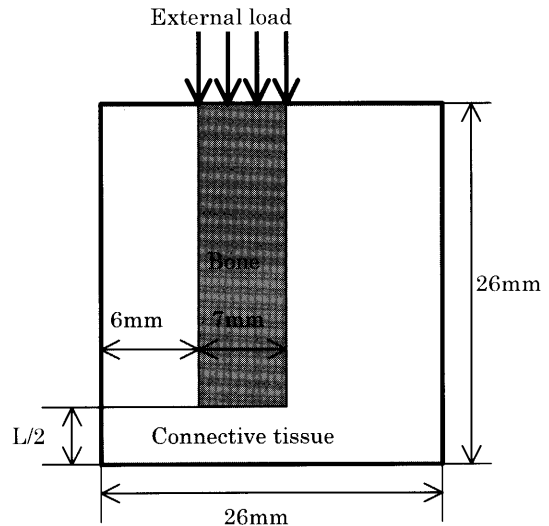


Fig. 5 Simulation region for human bone

Table 3 Properties of tissues for human

Tissue	Modulus of elasticity E [MPa]	Poisson's ratio ν
Bone	172000	0.3
Cartilage	10	0.35
Connective tissue	0.5	0.45

gap is perfectly replaced with bone. To define complete healing, as the first step, the simulation for a healthy bone model without fracture, as shown in Fig. 8, is performed and the deformation is obtained to be 0.001 9 mm. Consequently, in this study, the condition of complete healing is that the deformation becomes 0.002 1 mm, which is 10% greater than in the healthy case. However, even if the deformation satisfies this criterion, there is a possibility that the bone has not grown completely. Thus another criterion for complete healing is defined: the equivalent Young's modulus in the connective domain of 0.2 mm \times 7.0 mm, as shown in Fig. 9, becomes 4 300 MPa, which is 1/4 that for healthy bone. In this study, complete healing is when both criteria are satisfied.

The result for the reference case, $L = 3.0$ mm and $D_{\max} = 0.2$ mm, is checked using the criteria. Figure 10 shows the precise result of the static deformation and equivalent Young's modulus. The static deformation became smaller than 0.002 1 mm at 88 days, and the equivalent Young's modulus became greater than 4 300 MPa also at 88 days. As a result, complete healing is judged to be achieved at 88 days. This result agrees well with the actual healing result under clinical considerations.

4.3 Simulation results for various operation conditions

The influences of operation conditions, which are the initial gap and stopper gap, on the healing results are investigated. Reference conditions are $L = 3.0$ mm and

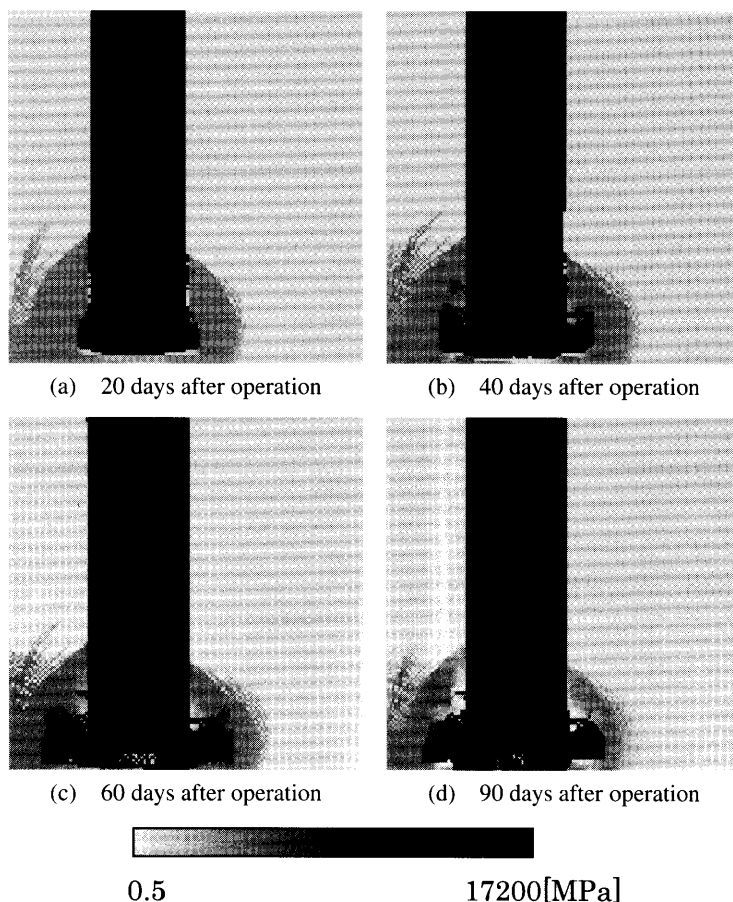


Fig. 6 Modulus of elasticity at sequential stages of fracture healing

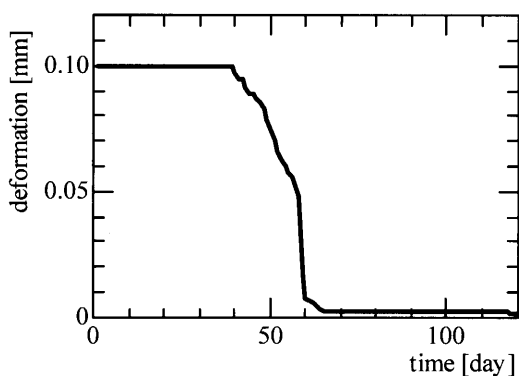
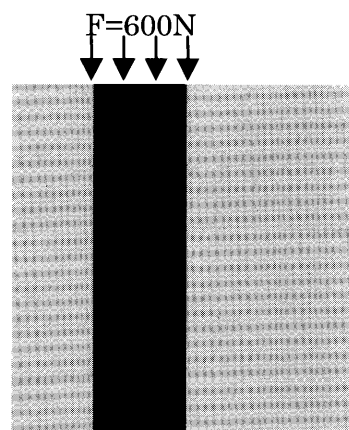
Fig. 7 Static deformation for the reference condition ($L=3.0$ mm, $D_{\max}=0.2$ mm)

Fig. 8 Simulation model for healthy bone

$D_{\max}=0.2$ mm, and values $2/3$ and $4/3$ the reference values are adopted. The parameters for simulation cases are shown in Table 4.

Case 1: $L=2.0$ mm and $D_{\max}=0.133$ mm

Under these conditions, the stopper gap is too narrow so that stimulus is insufficient in the gap region. As a result, new bone does not grow and static deformation does not decrease. Similar results can be seen for Case 2 and Case 3. From these results, it is considered that $D_{\max}=0.133$ mm is not an adequate operation condition.

Case 4: $L=2.0$ mm and $D_{\max}=0.2$ mm

The stopper gap and initial gap are narrow so that stimulus is insufficient in the gap region. Complete healing is attained at 116 days.

Case 5: $L=4.0$ mm and $D_{\max}=0.2$ mm

The initial gap is wide and the stopper gap is narrow so that stimulus is insufficient in the gap region. As a result, complete healing is attained at 106 days.

Case 6: $L=2.0$ mm and $D_{\max}=0.266$ mm

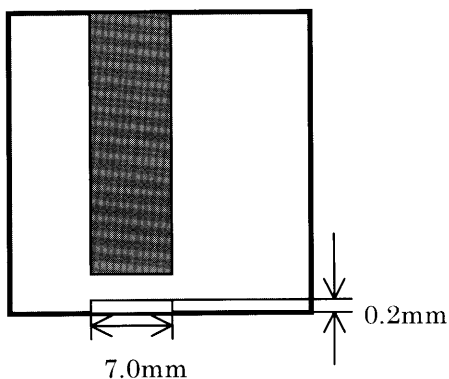
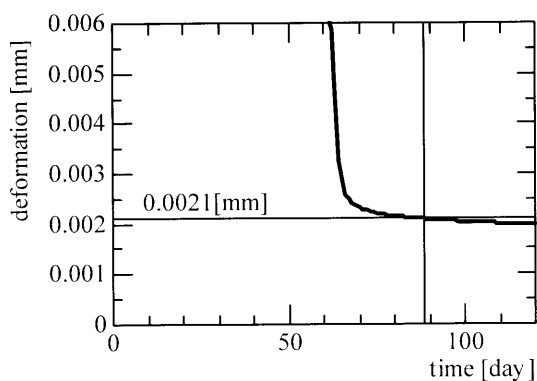
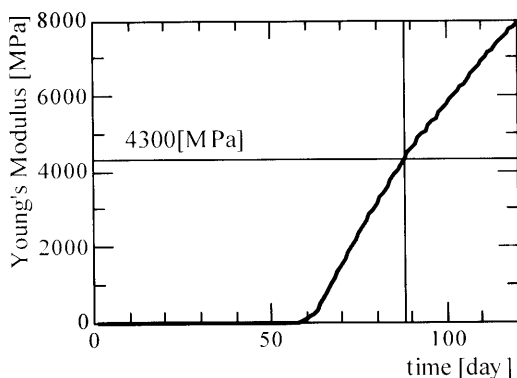


Fig. 9 Calculation region for equivalent Young's modulus



(a) Static deformation



(b) Young's modulus

Fig. 10 Precise result for the reference condition ($L = 3.0$ mm, $D_{max} = 0.2$ mm)

Table 4 Simulation conditions

		L (mm)		
		2.0	3.0	4.0
D_{max} (mm)	0.133	Case 1	Case 2	Case 3
	0.200	Case 4	Reference	Case 5
	0.266	Case 6	Case 7	Case 8

The initial gap is narrow but the stopper gap is adequate so that complete healing is attained at 88 days. These conditions are as good as the reference conditions. Case 7: $L = 3.0$ mm and $D_{max} = 0.266$ mm

The stopper gap is wide so that the stimulus is too strong in the initial stage of healing. As a result, new bone

Table 5 Periods for complete healing

“D” indicates the period from static deformation as well as “E” indicates the one from equivalent Young’s modulus.

		L (mm)		
		2.0	3.0	4.0
D_{max} (mm)	0.133	×	×	×
	0.200	116 days (D : 95) (E : 116)	88 days (D : 88) (E : 88)	106 days (D : 98) (E : 106)
	0.266	89 days (D : 84) (E : 89)	100 days (D : 100) (E : 96)	95 days (D : 95) (E : 85)

does not grow during this period, and complete healing is attained at 100 days.

Case 8: $L = 4.0$ mm and $D_{max} = 0.266$ mm

The initial gap is wide, as is the stopper gap, so an adequate stimulus can be obtained. As a result, complete healing is attained at 95 days.

4.4 Discussions

The simulation method of fracture healing during external fixation was applied to the healing of human bone. The influences of the operate conditions on the healing results were investigated. Complete healing was first defined using static deformation and equivalent Young’s modulus, and then bone healing was simulated under various initial gap and stopper gap values. The results are summarized in Table 5.

In the case of $D_{max} = 0.133$ mm, the stopper gap was too narrow so stimulus was insufficient and healing could not be achieved.

In the cases of $D_{max} = 0.2$ mm and 0.266 mm, healing was achieved. In this study, healing was achieved fastest in the case of $L = 3.0$ mm and $D_{max} = 0.2$ mm. There is a relationship between the initial gap and the stopper gap. When $L = 2.0$ mm or $L = 4.0$ mm, healing in the case of $D_{max} = 0.266$ mm was better than that in the case of $D_{max} = 0.2$ mm. However, when $L = 3.0$ mm, healing in the case of $D_{max} = 0.2$ mm was better than that in the case of $D_{max} = 0.266$ mm.

When the relationship between the stimulus and remodeling, from the clinical viewpoint, becomes further clarified, the local rules used in the CA method can be improved, and this simulation method will give useful information for actual operation.

5. Conclusions

In this study, fracture healing was simulated by the CA method. First, a set of local rules was constructed referring to the fuzzy logic model for sheep metatarsal. The simulation results obtained by the CA method agreed well with the ones in the previous research and the experimental data. As a result, it was concluded that the CA simulation model proposed in this study is a suitable model for

describing fracture healing. Next, modifying the parameters of local rules, fracture healing of human bone was simulated. On the basis of the simulation results obtained under various conditions of external fixation, it was concluded that healing is not achieved when the stopper gap is too narrow, and that an optimal set of stopper gap and initial gap conditions may exist because they have a close relationship to each other.

References

- (1) Carter, D.R., Blenman, P.R. and Beaupre, G.S., Correlations between Mechanical Stress History and Tissue Differentiation in Initial Fracture Healing, *Journal of Orthopaedics Research*, Vol.6 (1988), pp.736–748.
- (2) Carter, D.R., Beaupre, G.S., Giori, N.J. and Helms, J.A., Mechanobiology of Skeletal Regeneration, *Clinical Orthopaedics*, Vol.S355 (1998), pp.41–55.
- (3) Blenman, P.R., Carter, D.R. and Beaupre, G.S., Role of Mechanical Loading in Progressive Ossification of a Fracture Callus, *Journal of Orthopaedics Research*, Vol.7 (1989), pp.398–407.
- (4) Prendergast, P.J., Huiskes, R. and Soballe, K., Biophysical Stimuli on Cells during Tissue Differentiation at Implant Interfaces, *Journal of Biomechanics*, Vol.30 (1997), pp.539–548.
- (5) Claes, L.E., Heigele, C.A., Neidlinger-Wilke, C., Kaspar, D., Seidl, W., Margevicius, K.J. and Augat, P., Effects of Mechanical Factors on the Fracture Healing Process, *Clinical Orthopaedics*, Vol.S355 (1998), pp.132–147.
- (6) Claes, L.E. and Heigele, C.A., Magnitudes of Local Stress and Strain along Bony Surfaces Predict the Course and Type of Fracture Healing, *Journal of Biomechanics*, Vol.32 (1999), pp.255–266.
- (7) Alicia, B.-P. and Marjolein C.H. van der Meulen, Beneficial Effects of Moderate, Early Loading and Adverse Effects of Delayed or Excessive Loading on Bone Healing, *Journal of Biomechanics*, Vol.36 (2003), pp.1069–1077.
- (8) Lacroix, D. and Prendergast, P.J., A Mechano-Regulation Model for Tissue Differentiation during Fracture Healing: Analysis of Gap Size and Loading, *Journal of Biomechanics*, Vol.35 (2002), pp.1163–1171.
- (9) Gardner, T.N., Stoll, T., Marks, L., Mishra, S. and Knothe-Tate, M., The Influence of Mechanical Stimulus on the Pattern of Tissue Differentiation in a Long Bone Fracture — An FEM Study, *Journal of Biomechanics*, Vol.33 (2000), pp.415–425.
- (10) Gardner, T.N., Stoll, T., Marks, L., Knothe-Tate, M., Mishra, S., Evans, M., Simpson, H., Hardy, J. and Kenwright, J., A Finite Element Model of a Human Tibial Fracture. Stress Concentrations and Mechanical Failure in Healing Callus, *Journal of Biomechanics*, Vol.31 (1998), p.11.
- (11) Duda, G.N., Eckert-Hübner, K., Sokiranski, R., Kreutner, A., Miller, R. and Claes, L., Analysis of Inter-Fragmentary Movement as a Function of Musculoskeletal Loading Conditions in Sheep, *Journal of Biomechanics*, Vol.31 (1997), pp.201–210.
- (12) Duda, G.N., Kirchner, H., Wilke, H.-J. and Claes, L., A Method to Determine the 3-D Stiffness of Fracture Fixation Devices and Its Application to Predict Inter-Fragmentary Movement, *Journal of Biomechanics*, Vol.31 (1997), pp.247–252.
- (13) Ament, Ch. and Hofer, E.P., A Fuzzy Logic Model of Fracture Healing, *Journal of Biomechanics*, Vol.33 (2000), pp.961–968.
- (14) Kawamura, S., Kamitani, K., Iwatsubo, T., Matsuda, M. and Kurosaka, M., Adaptive Bone Remodeling Simulation by Using Cellular Automata, *Proc. of Int. Soc. of Biomechanics XVIII-th Congress*, Zuerich, (2001), on CD-ROM.
- (15) Tsubota, J., Kurosaka, M., Yamada, M., Nakabayashi, K., Mizuno, K., Iwatsubo, T. and Kawamura, S., Three Dimensional Finite Element Analysis of Impact Force Transmission in the Knee Joint, *Journal of Japanese Society for Clinical Biomechanics and Related Research*, (in Japanese), Vol.16 (1995), pp.461–464.